

University of Nebraska - Lincoln  
**DigitalCommons@University of Nebraska - Lincoln**

---

Civil Engineering Faculty Publications

Civil Engineering

---

2017

# Development of a Test Level 3 Transition Between Guardrail and Portable Concrete Barriers

Robert W. Bielenberg

*University of Nebraska - Lincoln*, rbielenberg2@unl.edu

David Gutierrez

*Gyrodata, Inc., Houston, TX*

Ronald K. Faller

*University of Nebraska - Lincoln*, rfaller1@unl.edu


John D. Reid

*University of Nebraska - Lincoln*, jreid@unl.edu

Phil Tenhulzen

*Nebraska Department of Roads*, Phil.tenhulzen@nebraska.gov

Follow this and additional works at: <http://digitalcommons.unl.edu/civilengfacpub>

 Part of the [Civil Engineering Commons](#), [Construction Engineering and Management Commons](#), [Engineering Science and Materials Commons](#), [Navigation, Guidance, Control, and Dynamics Commons](#), and the [Transportation Engineering Commons](#)

---

Bielenberg, Robert W.; Gutierrez, David; Faller, Ronald K.; Reid, John D.; and Tenhulzen, Phil, "Development of a Test Level 3 Transition Between Guardrail and Portable Concrete Barriers" (2017). *Civil Engineering Faculty Publications*. 138.  
<http://digitalcommons.unl.edu/civilengfacpub/138>

This Article is brought to you for free and open access by the Civil Engineering at DigitalCommons@University of Nebraska - Lincoln. It has been accepted for inclusion in Civil Engineering Faculty Publications by an authorized administrator of DigitalCommons@University of Nebraska - Lincoln.

Published in *Transportation Research Record: Journal of the Transportation Research Board*, No. 2638 (2017), pp 77–87.

doi 10.3141/2638-09

Published by SAGE Publications. Used by permission.

The Standing Committee on Roadside Safety Design peer-reviewed this paper.

---

## Development of a Test Level 3 Transition Between Guardrail and Portable Concrete Barriers

Robert W. Bielenberg,<sup>1</sup> David Gutierrez,<sup>2</sup> Ronald K. Faller,<sup>1</sup>  
John D. Reid,<sup>3</sup> and Phil Tenhulzen<sup>4</sup>

<sup>1</sup> Midwest Roadside Safety Facility, University of Nebraska–Lincoln,  
130 Whittier Building, 2200 Vine Street, Lincoln, NE 68583-0853

<sup>2</sup> Gyrodata, Inc., 4425 Jefferson Street, Houston, TX 77023

<sup>3</sup> Mechanical and Materials Engineering, Midwest Roadside Safety Facility,  
University of Nebraska–Lincoln, W342 NH, Lincoln, NE 68588

<sup>4</sup> Roadway Design Division, Nebraska Department of Roads,  
1500 Nebraska 2, Lincoln, NE 68502

*Corresponding author* — R. W. Bielenberg, rbielenberg2@unl.edu

### Abstract

Road construction often requires that work zones be created and shielded by portable concrete barriers (PCBs) to protect workers and equipment from errant vehicles as well as to prevent motorists from striking other roadside hazards. For an existing W-beam guardrail system installed adjacent to the roadway and near the work zone, guardrail sections are removed so a PCB system can be placed. A study was done to develop a crashworthy transition between W-beam guardrail and PCB systems. Design concepts were developed and refined through computer simulation with LS-DYNA. Additionally, a study of critical impact points was conducted to determine impact locations for full-scale crash testing. The design effort resulted in a new system consisting of a Midwest Guardrail System that overlapped a series of F-shape PCB segments placed at a 15:1 flare. In the overlapped region of the barrier systems, uniquely designed block-out supports and a specialized W-beam end shoe mounting bracket were used to connect the systems. Three full-scale vehicle crash tests were successfully conducted according to the *Manual for Assessing Safety Hardware* Test Level 3 safety performance criteria. Because of the successful test results, a Test Level 3 crashworthy guardrail-to-PCB transition system is now available for protecting motorists, workers, and equipment in work zones.

A transition between portable concrete barriers (PCBs) and W-beam guardrail is necessary when roadway construction requires that a work zone be created to shield workers and equipment from errant vehicles. For an existing W-beam guardrail system installed adjacent to the roadway and near the work zone, guardrail sections are removed so PCBs can be placed. If a proper transition is not installed, the region where the two barriers meet can create safety hazards, including the potential for poor vehicle capture, snagging on the end of the PCBs, and rapid vehicle deceleration.

The primary concerns associated with a connection between W-beam guardrail and PCBs correspond to the difference in barrier deflections and functionality of the barriers. Strong-post, W-beam guardrail systems have dynamic barrier deflections of approximately 40 in. for *Manual for Assessing Safety Hardware* (MASH) Test Level 3 (TL-3) impacts with passenger vehicles (1). However, freestanding PCB systems may have a dynamic barrier deflection as high as 80 in. under similar impact scenarios. Although a transition from guardrail to PCBs may not need to be as stiff as a conventional approach guardrail transition to bridge rails, it must provide sufficient lateral stiffness and strength to prevent pocketing as well as shield the end of the concrete barrier. Therefore, a proper transition in lateral barrier stiffness and strength is needed to connect the two systems. However, a crashworthy transition between guardrail and PCBs was unavailable.

To address this need, the Nebraska Department of Roads (NDOR) sponsored research to develop, test, and evaluate a transition system between W-beam guardrail and freestanding PCBs. This transition would significantly improve safety for the motoring public and work-zone workers through a combination of design, computer simulation, and full-scale crash testing. The transition system was to meet the TL-3 safety performance criteria set forth in MASH (1). The research focused on the F-shape PCB system developed through the Midwest States Pooled Fund Program and used by NDOR (2, 3).

## **Background**

A literature review of research related to W-beam guardrails, PCB systems, and transitions provided knowledge on barrier deflections and transitioning techniques. Individual barrier and transition system performance was reviewed with respect to vehicle snag, vehicle capture and stability, barrier pocketing, and barrier connection design. Full details about the literature search are available elsewhere (4, 5). A review of the two barrier types revealed that the F-shape PCB had almost two times the dynamic deflection of most W-beam guardrail systems. MASH TL-3 testing of the F-shape PCB

showed a maximum lateral dynamic barrier deflection of 79.7 in. (3). Similar testing of W-beam guardrail systems found an average dynamic deflection of 39.7 in. and 41.4 in. for guardrail systems 27 in. and 31 in. tall, respectively (6). System behavior differed for the two barriers. For W-beam guardrail, barrier deflections began immediately on impact, and peak dynamic deflection typically occurred when the vehicle was parallel with the barrier. However, PCB deflections were slower to develop because of the inertia of the PCB segments, and the peak deflection of the F-shape PCB occurred after the vehicle exited the barrier system as the segments continued to slide on the pavement.

### **Design Criteria**

Basic design criteria were developed to meet NDOR needs for barrier performance and future implementation and included the following:

1. The transition should meet MASH TL-3 while minimizing barrier pocketing, vehicle snag, vehicle instability, and rapid deceleration.
2. The preferred transition would accommodate existing G4(1S) guardrail systems (7). However, the 31-in.-tall Midwest Guardrail System (MGS) (8) was allowable if required.
3. Guardrail stiffening through reduced post spacing or PCB stiffening through anchorage was not desired.
4. The transition should consider reverse-direction impacts resulting from two-way traffic.
5. When transition installations occur near unpaved surfaces, PCBs will be installed on a compacted, crushed rock pad to mitigate barrier gouging in soil, tipping, and excessive rotation.

### **Development and Simulation of Transition Concepts**

A variety of transition concepts were formulated to meet the design criteria and were ranked by their feasibility, potential safety performance, and ease of installation. The transition should be easy to install and the number of additional components limited. Therefore, each concept was presented in its simplest form, and additional features were added, as needed, to improve performance.

A review of potential transition concepts focused the research on two preferred concepts, shown schematically in **Figure 1**:

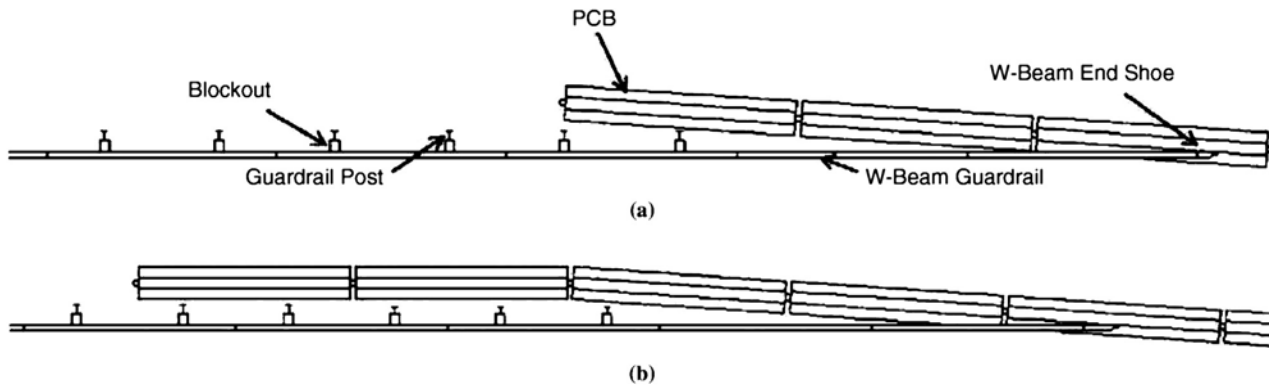


**Figure 1.** Preferred transition concepts: **(a)** flared PCB–modified G4(1S) and **(b)** parallel PCB–modified G4(1S).

1. Flared PCB, modified G4(1S): three 15H:1V flared PCB segments extended behind a modified G4(1S) guardrail system, posts interfering with installed PCB segments removed.
2. Parallel PCB, modified G4(1S): two PCB segments placed parallel to and behind a modified G4(1S) guardrail system before the PCB system was flared at 15H:1V to create a work zone.

### Simulation of Transition Concepts

LS-DYNA was used to analyze and refine the transition concepts (9). According to MASH TL-3, transitions must be impacted at a nominal speed of 62.1 mph and an angle of 25°. Therefore, each candidate design was subjected to simulated impacts according to these parameters and at several impact locations, ranging from the connection point between the guardrail and the PCB system to four posts upstream of the PCB system.

Criteria used in the analysis of the concepts included vehicle behavior, occupant risk, and rail pocketing. Vehicle behavior was examined to evaluate the potential for vehicle capture and redirection without vehicle instability. Vehicle snag on the upstream end of the PCB system or other transition components could affect vehicle stability and cause rapid deceleration. Occupant risk measures, including occupant impact velocities and occupant ridedown accelerations (ORAs), were evaluated to determine the degree of hazard to occupants in the impacting vehicle. Finally, rail pocketing angles above 23° were a concern for the transition as excessive

pocketing angles are associated with degraded barrier performance, including rail rupture (10).

LS-DYNA models of the freestanding F-shape temporary concrete barrier, modified G4(1S), and MGS were developed in previous studies (11, 12). A Chevrolet Silverado was chosen for the simulation study because of the likelihood of increased barrier deflections, rail and anchor loads, rail pocketing, and wheel snag with this vehicle type. Vehicle instabilities, related to vehicle climb, have been exhibited during full-scale crash tests involving 2270P pickup trucks with F-shape PCB systems. The Silverado vehicle model was created by the National Crash Analysis Center and later modified by Midwest Roadside Safety Facility personnel.

### **Concept 1: Flared PCB–Modified G4(1S) Simulation**

Analysis of the transition concepts began with simulation of Concept 1, the flared PCB–modified G4(1S) concept. Several variations of the concept were analyzed, starting with a basic overlapping and connection of the flared PCB and the guardrail, as shown in **Figure 1**. Subsequent modifications improved transition performance through the use of thrie beam, blockouts between the guardrail and PCB, addition of a cantilever beam off the end of the PCBs, and guardrail nesting.

A full discussion of the simulations is available elsewhere (4). Several notable conclusions drawn from the simulation of the flared PCB–modified G4(1S) concept are discussed here. First, the modified G4(1S) system lacked the height and stiffness to safely capture and redirect the vehicle, and problems with vehicle stability and barrier pocketing were noted at several impact points. A transition involving thrie beam upstream of the PCBs was simulated, yielding improved vehicle stability. However, the guardrail support posts tended to wedge against the PCBs, which led to elevated occupant risk values and rail pocketing angles. Thus, posts were removed and replaced with blockouts attached to the PCBs. Blockouts were installed at a standard post spacing of 6 ft 3 in. in the later configurations.

The fully blocked, thrie beam configuration yielded results with improved vehicle stability and occupant risk but with high rail pocketing angles. The pocketing behavior was caused by delayed displacement of the PCBs at the beginning of the impact event. Nested thrie beam was implemented to stiffen the guardrail system ahead of the PCB system and improve rail pocketing. The nested, fully blocked, thrie beam rail configuration yielded improved pocketing angles. A comparison of simulation results for the baseline flared PCB–modified G4(1S) concept and the improved design with nested, fully blocked, thrie beam rail is shown in **Figure 2**.

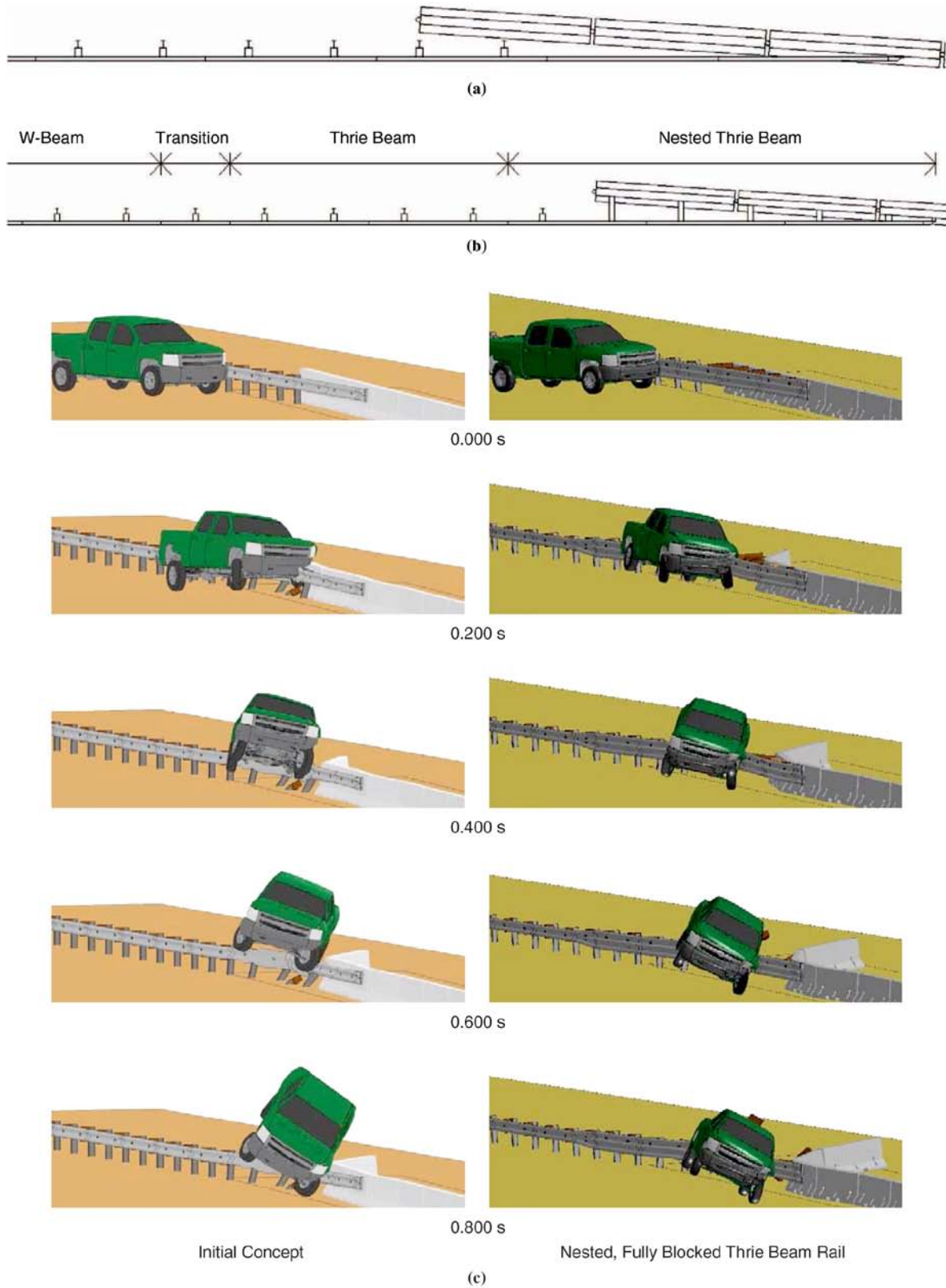


**Figure 2.** Comparison of flared PCB-modified G4(1S) simulation configuration: **(a)** initial flared PCB-modified G4(1S) concept; **(b)** flared PCB-modified G4(1S) concept with nested, fully blocked thrie beam rail; and **(c)** sequential comparison.

### **Concept 2: Parallel PCB–Modified G4(1S) Simulation**

Analysis of the transition concepts continued with simulation of Concept 2, the parallel PCB–modified G4(1S) concept, which used modified G4(1S) guardrail attached to F-shape PCBs with two segments installed parallel to and behind the guardrail system. Modifications were implemented into this concept on the basis of simulation results from the flared PCB–modified G4(1S) concept. Thus, nested thrie beam was installed for the final five rail sections in the transition adjacent to the PCBs, and the posts in front of the PCBs were removed and replaced with blockouts attached to the PCB segments at a standard spacing of 6 ft 3 in. The configuration of nested thrie beam with fully blocked rail yielded two marginal longitudinal ORA values but had acceptable vehicle stability and rail pocketing angles.

Review of the simulation results for the flared PCB–modified G4(1S) and parallel PCB–modified G4(1S) concepts showed that the nested thrie beam configurations with fully blocked-out rail for both transition concepts have potential to meet MASH TL-3. The parallel PCB configuration did not show any discernible benefit compared with a flared PCB configuration, so the flared configuration was preferred because of its reduced barrier overlap and simplicity. To address concerns that incorporation of thrie beam elements may be overly complex and labor-intensive, it was recommended that the modified G4(1S) be replaced with the MGS as a third design concept. It was anticipated that the 31-in. top mounting height of the MGS would aid in vehicle capture and redirection without a transition to thrie beam.

### **Concept 3: Flared PCB–MGS Simulation**

The flared PCB–MGS concept was similar to the flared PCB–modified G4(1S) concept, except MGS was connected to the 15H:1V flared PCB system in lieu of modified G4(1S). Although simulation results for the modified G4(1S) indicated that posts in front of PCBs would deform and wedge against the face of the PCB, the increased rail height of the MGS was thought to improve capture and redirection of the 2270P vehicle with reduced instabilities. Additionally, two posts remained in front of the first PCB segment and were intended to aid in PCB displacement. On impact, the posts were expected to rotate backward into the PCB and initiate displacement, which would reduce vehicle climb and instabilities.

Simulation results for the baseline flared PCB–MGS configuration yielded high occupant risk values because of vehicle snag, and pocketing angles were a concern for impacts upstream of the PCB system. Thus, modifications to the configuration were investigated to improve performance. Modified configurations were simulated with blockout variations and cantilever beams, but high pocketing angles continued to be a concern with the attachment



of the MGS to PCBs. To improve this behavior, a flared PCB–MGS configuration with nested rail placed upstream from and in front of the PCB system was simulated to stiffen the barrier system and lower pocketing angles. The simulation results for the nested-MGS configuration showed that occupant risk measures and pocketing angles were reduced to acceptable levels for all impact locations.

### **Concept Selection**

The simulation results from the flared PCB–modified G4(1S), parallel PCB–modified G4(1S), and flared PCB–MGS concepts were compared and used to select the transition configurations with the best performance. The compared metrics included occupant risk values, vehicle orientation angles to determine relative stability, vehicle snag, and barrier pocketing angles. The minimum value for each metric represented the safest transition design. The metrics that exceeded or were within 20% of MASH or recommended limits, practicality, and ease of installation were used to rank the configurations within each design concept as well as to establish whether each configuration had a high, moderate, or low likelihood of success. The comparison and rankings are shown in detail elsewhere (4).

According to the rankings, the flared PCB–MGS with nested rail configuration was preferred. It was the only configuration within all three concepts that did not raise concerns about degraded vehicle behavior and occupant risk or show high pocketing angles. Also, nesting of the MGS would not significantly increase installation effort compared with several other promising configurations, including a transition to thrie beam. Thus, the flared PCB–MGS configuration with nested rail was selected as the preferred alternative and recommended for full-scale crash testing and evaluation.

### **Selection of Critical Impact Points and Test Matrix**

According to MASH TL-3, transitions between longitudinal barrier systems must be subjected to two full-scale vehicle crash tests:

1. Test 3-20, impact with 1100C vehicle at critical impact points (CIPs) of the transition system at 62.1 mph and 25°.
2. Test 3-21, impact with 2270P vehicle at CIPs of the transition system at 62.1 mph and 25°.

Three crash tests were recommended for evaluating the transition system, including MASH Tests 3-20 and 3-21 to evaluate the transition with an 1100C

small car and a 2270P pickup truck. In addition, it was anticipated that a reverse-direction impact of Test 3-21 with the 2270P vehicle would be needed for evaluating the transition that would be subjected to two-way traffic adjacent to the barrier. Because the transition design involved two semirigid barrier systems and no stiffening of the systems as they approached each other, separate evaluation of the stiffness transition and the barrier connection point was not warranted.

Computer simulation was conducted to determine the CIPs. In this analysis, LS-DYNA simulation was used to select the critical attachment point between the MGS and PCB systems and the CIP for Test 3-21 with the 2270P vehicle for both oncoming and reverse-direction traffic. A full discussion of the CIP analyses is available elsewhere (4). The relevant conclusions are as follows:

1. The 2270P CIP for the transition from guardrail to PCB was identified as the center of the fifth guardrail post upstream of the W-beam end shoe attachment because this location generated the greatest barrier pocketing.
2. The 2270P CIP for a reverse-direction impact into the transition from PCB to guardrail was identified as 12.5 ft upstream of the W-beam end shoe connection to the PCB. This point was selected because it maximized the climb of the 2270P vehicle on the face of the PCB segment and caused concerns about vehicle capture on the W-beam rail as it traversed the system.

Selection of a CIP for Test 3-20 was based on engineering analysis and a review of previous MASH testing with the 1100C vehicle. Maximizing vehicle extension under the guardrail and simultaneous interactions with the PCB to promote wedging of the corner of the small car under the guardrail and between the two overlapping barrier systems were considered. This type of behavior promotes increases in vehicle deceleration, instability, and loading on the guardrail element. Previous testing of an MGS approach guardrail transition with a 4-in.-tall wedge-shaped curb demonstrated that combined loading caused by the front corner of the vehicle being wedged vertically between the curb and the guardrail was sufficient to result in rail rupture (13). A review of this approach guardrail transition and other full-scale crash tests indicated that the CIP selected for Test 3-20 was 93¾ in. upstream of the second guardrail splice upstream of the end shoe connection. This selection ensured that the vehicle critically loaded a splice while being engaged with a W-beam guardrail and PCBs. Additionally, this CIP evaluated a potential for nondesirable vehicle interaction with the W-beam end shoe mounting bracket.

### Final Transition Details

The final transition comprised a tangent, nested MGS that overlapped an adjacent PCB system oriented at a 15:1 flare, as shown in **Figure 3**. Minimum installation recommendations for testing and evaluating the transition were based on the initial computer simulation analysis and consisted of the following:

1. For testing purposes, the transition should consist of at least a 137.5-ft-long MGS system and an 11-segment PCB system positioned at a 15H:1V flare.
2. The transition required a minimum of three PCB segments extending behind the nested MGS at a 15:1 flare, which corresponded to guardrail attachment to the upstream end of the fourth PCB segment. Additional PCBs flared behind the MGS would not be an issue because the potential for vehicle and barrier interaction with the PCBs was maximized for the minimum overlap condition.
3. Placement of standard MGS posts and blockouts was not recommended within the first two sections of guardrail upstream from the W-beam end shoe connection because the PCBs would interfere with existing posts. Thus, the connection between the guardrail and the PCB segments would use specially designed blackout mounts.
4. A minimum of five nested W-beam sections 12 ft 6 in. long were used upstream of the end shoe connection to the PCB. For the minimum PCB overlap noted above, this corresponds to one complete 12.5-ft-long section of nested rail upstream of the end of the PCBs.

The MGS was constructed with 16 steel posts spaced at 75 in. on center. The line posts were W6 × 8.5 sections with an embedment depth of 40 in. A blackout 6 in. wide by 12 in. deep by 14 in. long was used to block the rail away from the front face of each steel post. The 12-gauge W-beam was mounted at a height of 31 in. and nested for the first five 12.5-ft-long rail sections upstream of the W-beam end shoe. A tangent anchorage system was used on the upstream end of the MGS.

Eleven 12.5-ft-long F-shape PCBs were connected to the MGS system with a stiffness transition. The concrete barriers were 22 in. wide at the base and 8 in. wide at the top. Each barrier segment was interconnected by 1¼-in.-diameter A36 steel connection pins and connector plates placed between ¾-in.-diameter reinforcing loop bars extending from the end of the barrier sections. All PCB segments were set on a 6-in.-deep compacted crushed limestone pad meeting AASHTO Grade B soil specifications or were set on the concrete tarmac.

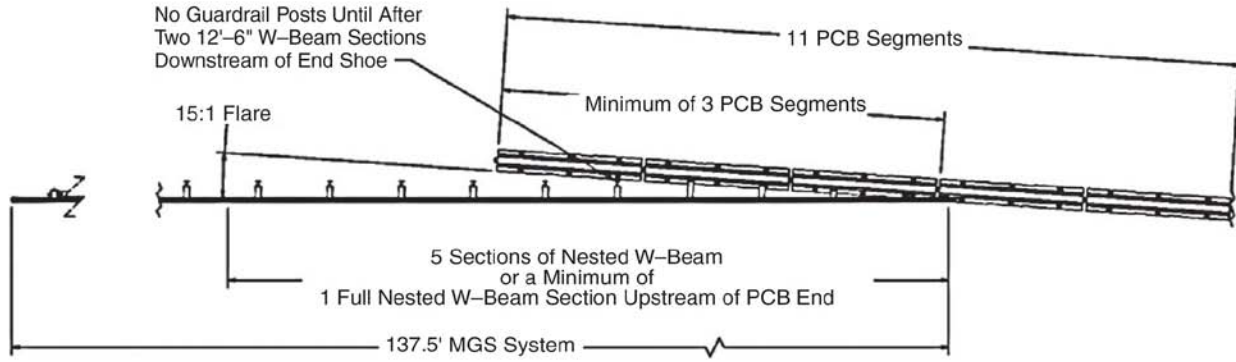


**Figure 3.** Guardrail-to-PCB transition system.

The overlapped portion of the transition from MGS to PCB incorporated four blockouts between the guardrail and Concrete Barriers 2 and 3 mounted on bent plate blockout attachments. The bent plate blockout attachment accounted for the vertical flare of the PCB, and individual timber blockouts were then cut on one face to match the offset depth and 15:1 flare of the PCB segments. Although the mounting plate had four holes, it was secured to the PCB using only two  $\frac{3}{4}$ -in.-diameter, 6-in.-long Powers wedge bolts. The additional holes provide an alternative for improper anchor installation or rebar interference. The bracket allowed for guardrail to be bolted to the blockout with guardrail bolts.

The guardrail was connected and transitioned to the concrete barrier at a  $3.8^\circ$  angle with a steel mounting bracket and W-beam end shoe. The basic design of the W-beam end shoe mounting bracket was similar to that of attachments previously developed for attachment of thrie beam approach guardrail transitions to sloped concrete parapets. The steel mounting bracket was mounted on the impact side of the fourth PCB segment and 10 in. from the upstream end with four 1-in.-diameter A325 Grade A bolts. The downstream end of the bracket was angled  $8.0^\circ$  to be flush against the concrete barrier. A W-beam end shoe was attached to the front of the connector plate with five  $\frac{7}{8}$ -in.-diameter A325 bolts secured by A563 nuts welded to the interior of the connection plate.

### **Test MGSPCB-1, MASH 3-21**

In Test MGSPCB-1, a 4,914-lb pickup truck impacted the PCB-to-MGS transition at a speed of 63.2 mph and an angle of  $25.3^\circ$ , as shown in Figure 4. Initial vehicle impact occurred 2.5 in. downstream of the fifth guardrail post upstream of the W-beam end shoe. The vehicle was captured by the W-beam rail element and redirected. No vehicle snag on the PCB system was observed. The vehicle snagged on the second and third posts upstream of the W-beam end shoe because the post deflected backward and against the first PCB segment, but the vehicle continued to be safely redirected. At 0.224 s after impact, the vehicle became parallel to the barrier. At 0.520 s, the vehicle exited the system. The vehicle came to rest 234 ft 1 in. downstream of the impact and 21 ft 11 in. in front of the barrier, and its trajectory did not violate the bounds of the exit box.

Barrier damage was moderate and consisted of rail deformation, damaged timber blockouts, bending of steel posts, contact marks on the front face of the concrete segments, and spalling of the concrete, as shown in **Figure 4**. Five of the guardrail posts were deformed, and the third post downstream of the impact point was twisted and bent downstream with the downstream side of the post against the upstream face of first PCB segment.





**Figure 4.** Test MGSPCB-1: (a) sequential events, (b) barrier damage, and (c) vehicle damage.

Contact marks from the vehicle were visible on the front face of the first two PCB segments, but no contact was noted with the upstream end of the first PCB. The blockout mounts and the W-beam end shoe mounting bracket were undamaged. The maximum lateral dynamic deflections were 36.1 in. for the rail, 27.7 in. at the first post downstream of impact, and 6.7 in. at the downstream end of the first PCB segment. The working width of the system was 58.7 in.

Exterior vehicle damage was moderate and concentrated on the right front corner and right side of the vehicle, where the impact occurred, as shown in Figure 4. Deformations of the interior occupant compartment were minimal and did not violate the limits established by MASH. All occupant risk measures were below the required values, and vehicle stability was acceptable. A longitudinal ORA of 20.34 *g* occurred because of vehicle snag on system posts that were deflected against the first PCB segment. Test MGSPCB-1 was determined to be acceptable according to the MASH TL-3 safety performance criteria.

### **Test MGSPCB-2, MASH 3-20**

In Test MGSPCB-2, a 2,436-lb car impacted the PCB-to-MGS transition at a speed of 65.1 mph and an angle of 24.0°, as shown in **Figure 5**. Initial vehicle impact occurred 99.5 in. upstream of the centerline of the second splice upstream of the W-beam end shoe. The vehicle was initially captured by the W-beam rail element and began to be redirected. The vehicle bumper, right front fender, and right front tire extended under the W-beam rail and impacted the second PCB segment in the system 0.060 s after impact, but the vehicle continued to be safely redirected as it engaged the two overlapped barrier systems. At 0.232 s after impact, the vehicle became parallel to the barrier. At 0.437 s, the vehicle exited the system. The vehicle came to rest 157 ft 5 in. downstream of the impact and 22 ft in front of the barrier oriented downstream, and its trajectory did not violate the bounds of the exit box.

Barrier damage was moderate and consisted of rail deformation, damaged timber blockouts, contact marks on the front face of the concrete segments, and spalling of the concrete barriers, as shown in Figure 5. The blockout mounts and the W-beam end shoe mounting bracket were undamaged. The maximum lateral dynamic deflections were 26.3 in. for the rail, 3.1 in. at the first post upstream of impact, and 28.1 in. at the downstream end of the second concrete barrier segment. The working width of the system was 61.4 in.

Exterior vehicle damage was moderate and was concentrated on the right front corner and right side of the vehicle, where the impact occurred, as shown in Figure 5. The windshield was deformed and shattered and had

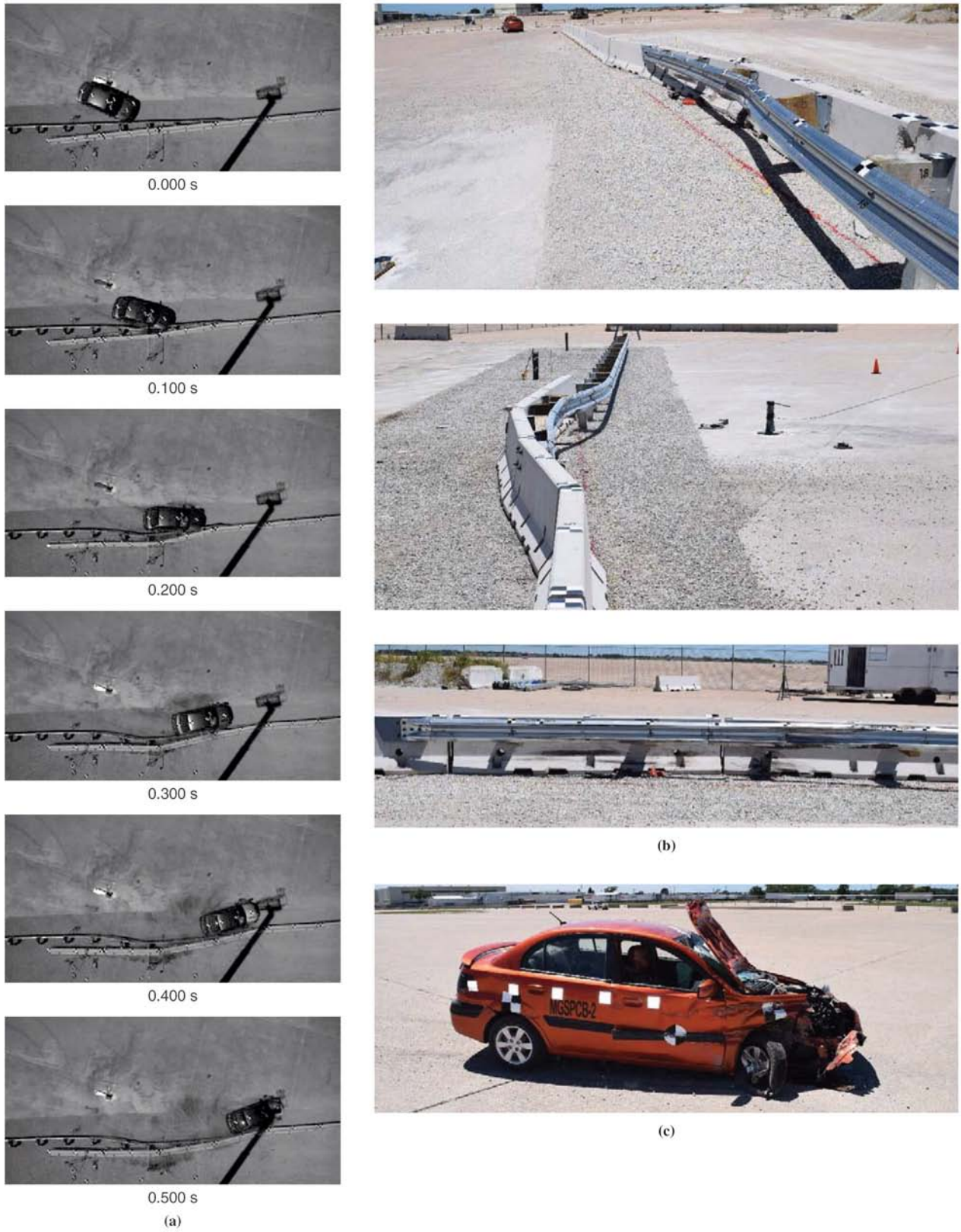


**Figure 5.** Test MGSPCB-2: (a) sequential events, (b) barrier damage, and (c) vehicle damage.



a 23-in.-long tear at the top located 10 in. from the left A pillar, caused by deployment of the front passenger airbag and its contact with the windshield. Because the damage was not related to vehicle interaction or direct contact with the barrier system, it was not considered in the test evaluation. Deformations of the interior occupant compartment were minimal and did not violate the limits established by MASH. All occupant risk measures were below the required values, and vehicle stability was acceptable. Test MGSPCB-2 was determined to be acceptable according to the MASH TL-3 safety performance criteria.

### **Test MGSPCB-3, MASH 3-21, Reverse Direction**

In Test MGSPCB-3, a 5,012-lb pickup truck impacted the PCB-to-MGS transition at a speed of 63.1 mph and an angle of 24.6°, as shown in **Figure 6**. The vehicle impacted 12 ft 9 in. upstream of the centerline of the W-beam end shoe on the fifth PCB segment in the system and began to be redirected. By 0.144 s, the right front fender contacted the leading edge of the W-beam end shoe mounting bracket, and the vehicle began to interact with the W-beam rail. A portion of the right front fender and right door snagged on the mounting bracket, but the vehicle continued to be safely redirected. At 0.192 s after impact, the vehicle became parallel to the barrier. At 0.606 s, the vehicle exited the system. The vehicle came to rest 187 ft 9 in. downstream of impact and 56 ft 10 in. behind the barrier oriented with the front of the vehicle facing away from the back of the barrier, and its trajectory did not violate the bounds of the exit box.

Barrier damage was moderate and consisted of cracking of the concrete, contact marks on the front and top faces of the concrete segments and the face of the W-beam rail, spalling of the concrete, damaged timber blockouts, and W-beam rail deformation, as shown in Figure 6. The first two impacted PCB segments displayed vertical cracking on the front and back faces of the barriers and minor concrete spalling. Only minor damage was noted to the remaining PCB segments. The blockout mounts and the end shoe mounting bracket were undamaged, except for minor scuff marks on the end shoe mounting bracket. The maximum lateral dynamic deflection of the rail and concrete barriers for the system was 30.6 in. for the rail and 37.2 in. at the upstream target on the second impacted concrete barrier segment. Guard-rail post motion was negligible. The working width of the system was 58.7 in.

Exterior vehicle damage was moderate and concentrated on the right front corner and right side of the vehicle, where the impact occurred, as shown in Figure 6. Deformation and tearing of the right front fender and right-side doors occurred because of snagging on the leading edge of the W-beam end shoe mounting bracket. The right fender was bent upward 9

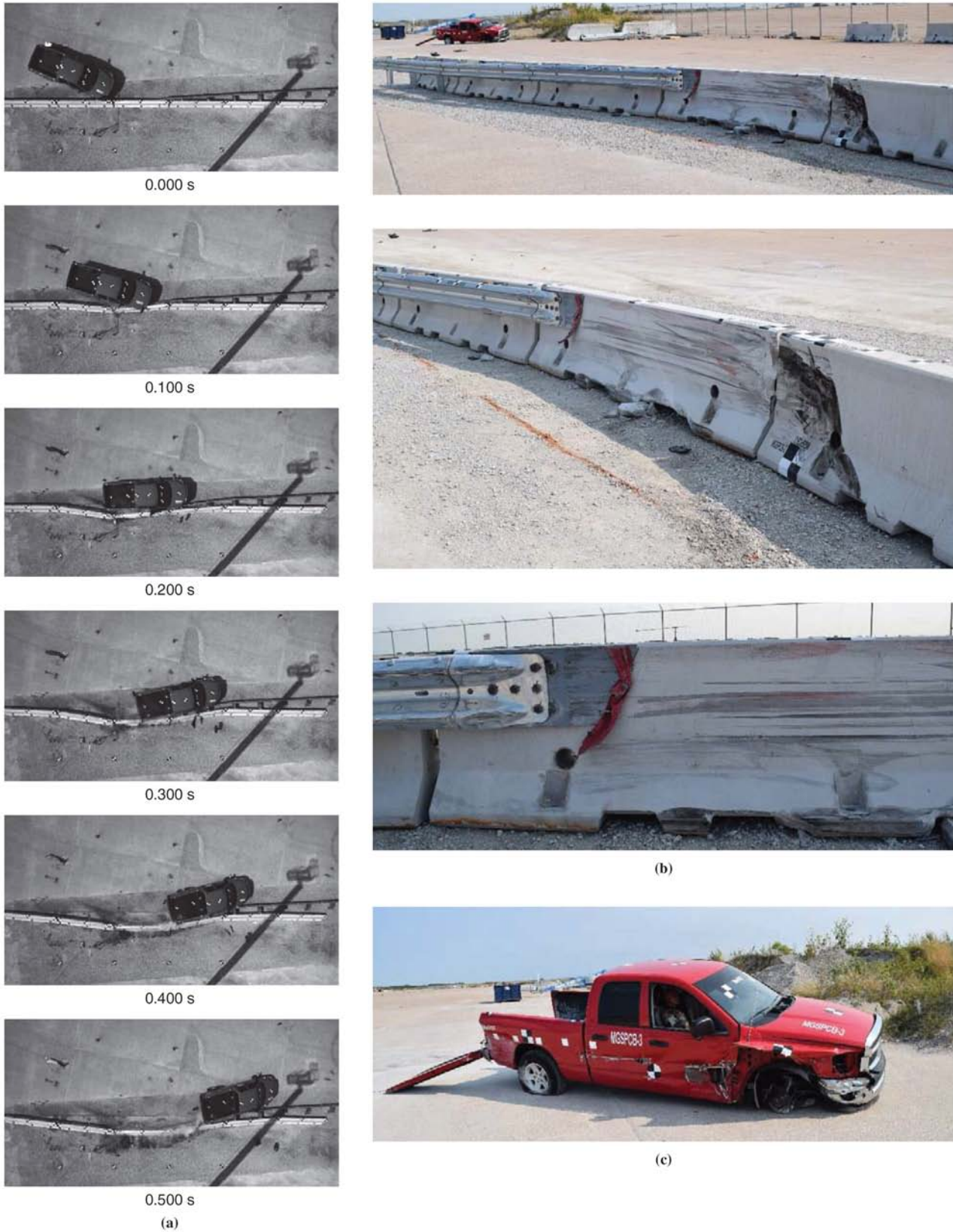


**Figure 6.** Test MGSPCB-3: (a) sequential events, (b) barrier damage, and (c) vehicle damage.

in. from the top edge of the wheel well, starting at the back of the fender and extending 20 in. forward. The right front door had a 23-in.-tall by 15-in.-wide tear at the front, 11 in. from the bottom, and the right rear door had an 8-in.-long by 3-in.-tall tear 17 in. from the bottom. The tears in the door were to the exterior sheet metal only and did not compromise the occupant compartment. Deformations of the interior occupant compartment were minimal and did not violate the limits established by MASH. All occupant risk measures were below the required values, and vehicle stability was acceptable. Test MGSPCB-3 was determined to be acceptable according to the MASH TL-3 safety performance criteria.

### **Summary, Conclusions, and Recommendations**

A crashworthy transition between guardrail and free-standing PCB was designed, tested, and evaluated under the safety requirements for MASH TL-3. The guardrail-to-PCB transition system was developed with extensive LS-DYNA simulation that investigated and refined potential concepts. Concepts were modified to enhance vehicle stability and to capture as well as mitigate occupant risk, vehicle snag, and barrier pocketing. Concept refinement led to a transition system comprising a tangent, nested MGS that overlapped an adjacent, flared PCB system. LS-DYNA simulation was also used to identify CIPs for full-scale crash testing.

The transition system was subjected to three full-scale crash tests and successfully evaluated according to MASH TL-3 impact safety standards. These tests evaluated structural integrity, vehicle snag, vehicle instability, and vehicle capture. The MASH TL-3 transition now provides the first crashworthy option to connect the MGS and F-shape PCBs. The transition design should be easy to implement because it requires minimal alterations of the guardrail and PCBs.

As with any new barrier system, design of the guardrail-to-PCB transition had to consider implementation guidance and provide recommendations for real-world installations. The recommended minimum system configuration for real-world installations is as follows:

1. A minimum 137.5-ft-long MGS system and an 11-segment PCB system at a 15H:1V flare should be used. A minimum of eight PCBs should be placed downstream of the point where the W-beam guardrail attaches to the PCBs. Shorter lengths for either barrier would need further evaluation.
2. The transition requires a minimum of three PCB segments extending behind the nested MGS at the 15H:1V flare, which allows anchorage

of the guardrail to the upstream end of the fourth PCB segment. Additional length of overlapped, flared PCB is acceptable.

3. For adequate anchorage of the end shoe mounting bracket on the PCB, the anchor bracket mounting bolts that extend through the PCB must be mounted a minimum of 12. in. from the upstream edge of the PCB segment, similarly to the full-scale crash testing detailed here.
4. A minimum of five 12.5-ft-long, nested W-beam sections must be used upstream of the end shoe connection to the PCBs.
5. The 15H:1V flare used in the transition to offset the PCBs behind the guardrail likely will convert to PCBs tangent to the roadway once the work zone has been established. Conversion from the 15H:1V flare to tangent to the roadway should not begin until a minimum of two PCB segments downstream from the W-beam end shoe connection.

Additional recommendations for grading, surfacing, and clear areas behind the transition as well as system repair guidance are provided elsewhere (5). The guardrail-to-PCB transition presented here focused on the MGS guardrail system and 12.5-ft-long, F-shape PCBs. Although the transition was designed specifically for these two barrier systems, there may be a need to integrate this transition with other barrier systems, including existing G4(1S) W-beam guardrail or alternative PCB designs. Guidance is provided by Lingenfelter et al. for transitioning from existing G4(1S) systems to the MGS in advance of the transition (5). Additionally, the transition could be adapted to other systems with considerations for barrier segment capacity, joint design, barrier geometry, and other factors. However, further research and testing likely would be needed to evaluate safety performance.

**Acknowledgments** — The authors acknowledge the Nebraska Department of Roads and the Smart Work Zone Deployment Initiative for sponsoring and guiding the project. The simulation was conducted at the Holland Computing Center at the University of Nebraska.

## References

1. *Manual for Assessing Safety Hardware*. AASHTO, Washington, D.C., 2009.
2. Faller, R. K., J. R. Rohde, B. T. Rosson, R. P. Smith, and K. H. Addink. *Development of a TL 3 F Shape Temporary Concrete Median Barrier*. Project SPR 3(017), Report TRP 03 64 96. Midwest Roadside Safety Facility, University of Nebraska–Lincoln, 1996.

3. Polivka, K. A., R. K. Faller, D. L. Sicking, J. R. Rohde, B. W. Bielenberg, J. D. Reid, and B. A. Coon. *Performance Evaluation of the Free-Standing Temporary Barrier—Update to NCHRP 350 Test No. 3-11 with 28" C.G. Height* (2214TB-2). Report TRP-03-174-06. Midwest Roadside Safety Facility, University of Nebraska–Lincoln, 2006.
4. Gutierrez, D. A., R. W. Bielenberg, R. K. Faller, J. D. Reid, and K. A. Lechtenberg. *Development of a Mash TL-3 Transition Between Guardrail and Portable Concrete Barriers*. Report TRP-03-300-14. Midwest Roadside Safety Facility, University of Nebraska–Lincoln, 2014.
5. Lingenfelter, J. L., J. E. Kohtz, R. W. Bielenberg, R. K. Faller, and J. D. Reid. *Testing and Evaluation of MASH TL-3 Transition Between Guardrail and Portable Concrete Barriers*. Draft Report TRP-03-335-16. Midwest Roadside Safety Facility, University of Nebraska–Lincoln, 2016.
6. Abu-Odeh, A. Y., K. M. Kim, and R. P. Bligh. *Guardrail Deflection Analysis, Phase I: (2010–2011)*. Report 405160-24. Texas Transportation Institute, College Station, 2011.
7. Bullard, D. L., W. L. Menges, and D. C. Alberson. *NCHRP Report 350 Compliance Test 3-11 of the Modified G4(1S) Guardrail with Timber Blockouts*. FHWA-RD-96-175. Texas Transportation Institute, College Station, 1996.
8. Faller, R. K., K. A. Polivka, B. D. Kuipers, R. W. Bielenberg, J. D. Reid, J. R. Rohde, and D. L. Sicking. Midwest Guardrail System for Standard and Special Applications. *Transportation Research Record: Journal of the Transportation Research Board*, No. 1890, 2004, pp. 19–33.
9. Hallquist, J. O. *LS-DYNA Keyword User's Manual*. Livermore Software Technology Corporation, Livermore, Calif., 2007.
10. Polivka, K. A., R. K. Faller, J. D. Reid, D. L. Sicking, J. R. Rohde, and J. C. Holloway. *Crash Testing of Missouri's W-Beam to Thrie Beam Transition Element*. Report TRP-03-93-00. Midwest Roadside Safety Facility, University of Nebraska–Lincoln, 2000.
11. Bielenberg, R. W., T. E. Quinn, R. K. Faller, D. L. Sicking, and J. D. Reid. *Development of a Retrofit, Low-Deflection, Temporary Concrete Barrier System*. Report TRP 03-295-14. Midwest Roadside Safety Facility, University of Nebraska–Lincoln, 2014.
12. Julin, R. D., J. D. Reid, R. K. Faller, and M. Mongiardini. *Determination of the Maximum MGS Mounting Height—Phase II Detailed Analysis Using LS-DYNA*. Report TRP-03-274-12. Midwest Roadside Safety Facility, University of Nebraska–Lincoln, 2012.
13. Winkelbauer, B. J., J. G. Putjenter, S. K. Rosenbaugh, K. A. Lechtenberg, R. W. Bielenberg, R. K. Faller, and J. D. Reid. *Dynamic Evaluation of MGS Stiffness Transition with Curb*. Report TRP 03-291-14. Midwest Roadside Safety Facility, University of Nebraska–Lincoln, 2014.